An Experimental Comparison of Mapping Methods, the Gutmann dataset

Arnoud Visser   David de Bos   Hessel van der Molen

Abstract— **A classical experiment is the sequence of papers based on the Radish dataset published by Steffen Gutmann. These papers were the basis of the Markov and Gaussian Localization chapter of the textbook 'Probabilistic Robotics'. The same dataset can be used for simultaneous localization and mapping, when the locations of the landmarks are not longer given. This gives a nice benchmark, with a very manageable set of landmarks (six) and realistic noise for both the movement and observation model of the Aibo robot. This paper describes a comparison of a number of well known simultaneous localization and mapping algorithms, including the details to get these algorithms working for this dataset.**

I. INTRODUCTION

Localization and mapping are essential capabilities of a mobile robot. After a classical survey [1], several algorithms were described in the textbook 'Probabilistic Robotics' [2]. Localization with an Extended Kalman Filter plays a central role in the textbook. This is partly because it is a textbook; the problem can be easily described with this algorithm. On the other hand, the Extended Kalman Filter is also a very robust and efficient algorithm; which allows it to be implemented on embedded processors with moderate resources.

Inside the textbook the example is used of a RoboCup soccer field, with several colored landmarks surrounding the field. This example was studied by one of the authors of the textbook; Dieter Fox [3]. The dataset was archived by Steffen Gutmann at the robotics data set repository Radish[1]. In this study a comparison was made between four localization methods: Markov-Kalman Localization, Sensor Resetting Localization, Mixture Monte Carlo Localization and Adaptive Monte Carlo Localization. This comparison (based on the same dataset) was later extended [4] with Multi Hypothesis Localization (also described in [2]).

Also inside the RoboCup this comparison and this dataset is often used. In the RoboCup competition efficiency and robustness are important capabilities. In addition, the rules of RoboCup allow a limited number of landmarks with a clear signature to be present around the field. A major limitation for Kalman Filters is the scaling of algorithm with respect to the number of landmarks, but the handful of landmarks around the field is easy to manage. Examples of teams who refer to this work are UChile [5], Cerberus [6], MetroBots [7] and the UW Huskies[8].

The RoboCup soccer field is a natural testbed for localization experiments. Mapping experiments seem to be a bit

artificial in this setting, because the location of the landmarks is clearly stated in the rules. Dellaert is the first to experiment with landmark-based SLAM and Aibos [9], although they directly complicated the scenario by using 32 landmarks and 10 robots. In this paper the original scenario is used, with only 6 landmarks and a single robot. The apriori knowledge about the location of the 6 landmarks is forgotten and only used in the evaluation of the different mapping algorithms. In this way an ideal testbed is created, which could be used for rapid prototyping. Adapting a mapping algorithm to this scenario seems simple, but requires the correct setting of both the motion and observation model. If a mapping algorithm fails for this simple scenario, the assumptions on the motion and observation should be adjusted. Although the scenario is simple, the dataset is challenging enough, with many artifacts in both the movements of the Aibo and the observations of the landmarks with the camera in the nose of the robot.

II. RELATED WORK

Peralta-Cabezas *et. al* [5] made a quite extensive comparison of Bayesian prediction techniques for localization in the RoboCup Small Size League. Their conclusion was that a classical Extended Kalman Filter and Particle Filter yielded as accurate results as more advanced algorithms with significantly less computational effort. Another observation was that the inclusion of an Improbability Filter [10] allowed for significant prediction improvements for all filters. This is in accordance with the analysis of Kristensen *et. al* [4], which report major improvements when using a *validation gate* [11], [12]. This *validation gate* is based on the same Mahalanobis distance criterion [13] as the Improbability Filter.

In contrast with localization experiments, mapping experiments with legged Aibo robots and a limited number of landmarks with known signature are not often performed. A nice experiment is performed by Dellaert *et. al* [9], where a hallway of colored cylinders is build on a 5x5m field. There were 32 cylinders, each cylinder with a unique color-coding. Multiple robots were present in the hallway (each walking 3m back and forth). A map of the environment was built in a distributed way, not by exchanging observations, but by exchanging updates of a clique tree. Yet, Dellaert's article describes only a single method. To the best of our knowledge no experimental comparison of mapping algorithms for the same scenario has been made.

Intelligent Systems Laboratory Amsterdam, Universiteit van Amsterdam, Science Park 904, 1098 XH Amsterdam, The Netherlands

[1]http://radish.sourceforge.net/

III. SIMULTANEOUS LOCALIZATION AND MAPPING METHODS

Three classical Simultaneous Localization and Mapping (SLAM) algorithms are compared:

A. SLAM with a Extended Kalman Filter

First implementations of EKF-SLAM were due to Moutarlier *et. al* [14] and Leonard *et. al* [15]. In this paper, the notation from the textbook [2] is followed. Simultaneous Localization and Mapping can be done by calculating an estimate of the posterior $p(x_t, m|z_{1:t}, u_{1:t})$ for both the current position x_t and the map m when the previous observations $z_{1:t}$ and motion updates $u_{1:t}$ are given. A Kalman Filter maintains a belief $\bar{y}_t$ of a state space y_t with an estimate of the mean vector $\bar{\mu}_t$ and a covariance matrix $\bar{\Sigma}_t$. In this case the state space $y_t = (x_t m)^T$; the combination of the robot pose x_t and the map m. The map m is represented with the location $m_{i,x}, m_{i,y}$ and signature s_i of each of the landmarks. In this experiment the number of landmarks is six, so the dimension of the state vector is $3 + 6 * 3 = 21$ elements long.

A Kalman Filter needs two models to update its beliefs; a motion model $p(x_t|u_t, x_{t-1})$ and a measurement model $p(x_t|z_t)$.

For the Aibo legged robot Gutmann *et al.* [3] used a motion model which was purely probabilistic; they combined three error sources: correct displacement with Gaussian noise, a uniform distribution due to obstructions and a random displacement due to kidnapping. Here, a motion model is used equivalent with the velocity model described in [2]:

$$\begin{pmatrix} x' \\ y' \\ \theta' \end{pmatrix} = \begin{pmatrix} x \\ y \\ \theta \end{pmatrix} + \begin{pmatrix} -\frac{\hat{v}}{\hat{\omega}} \sin \theta + \frac{\hat{v}}{\hat{\omega}} \sin (\theta + \hat{\omega}\Delta t) \\ \frac{\hat{v}}{\hat{\omega}} \cos \theta - \frac{\hat{v}}{\hat{\omega}} \cos (\theta + \hat{\omega}\Delta t) \\ \hat{\omega}\Delta t \end{pmatrix} + \mathcal{N}(0, R_t) \tag{1}$$

where the new pose $x_t = (x' \, y' \, \theta')^T$ is the result of applying the motion update $u_t = (v \, \omega)^T$ at the previous pose $x_{t-1} = (x \, y \, \theta)^T$. Here R_t is the uncertainty in the motion model, which is represented as the covariance of the Gaussian distribution $\mathcal{N}$. Such a motion model with a longitudinal speed v and turning speed ω seems inappropriate for a walking robot, but actually the interface to the Aibo consists of walk and turn commands which fit very well with this motion model.

The observation model is based on a model of landmark observations z_t consisting of a range r_t^i, a bearing ϕ_t^i and a signature s_t^i of a landmark i relative to the robot's local coordinate frame. The landmarks in this case are six color coded tubes, surrounding the field (See Fig. 1).

The landmarks are recognized by processing the images in the nose of the Aibo robot. The camera of the Aibo robot has a limited field of view, so in most cases only a single landmark is seen. The robot constantly scans the horizon with its head, what means that even when the robot remains long enough at the same location, a number of landmarks
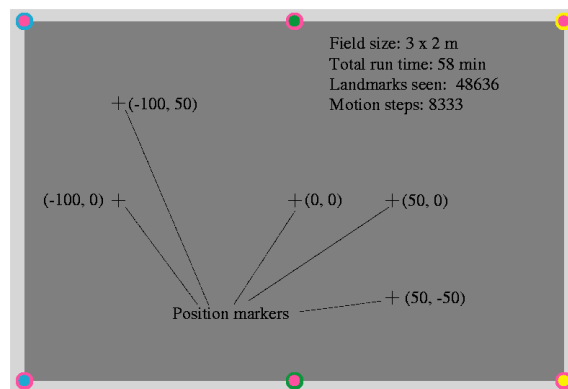

Fig. 1: The setup of the field, including six landmarks and the turning points on the field (Courtesy Gutmann[3]).

can be seen sequentially. The position of the robots head is already included in the range and bearing observation. This results in the following measurement model:

$$\begin{pmatrix} r_t^i \\ \phi_t^i \\ s_t^i \end{pmatrix} = \begin{pmatrix} \sqrt{\delta_x^j \cdot \delta_x^j + \delta_y^j \cdot \delta_y^j} \\ \text{atan2}(\delta_y^j, \delta_x^j) - \theta' \\ m_{j,s} \end{pmatrix} + \mathcal{N}(0, Q_t) \tag{2}$$

with $\delta_x^j = \bar{\mu}_{j,x} - x'$ and $\delta_y^j = \bar{\mu}_{j,y} - y'$ the x,y-components of the difference between the current position of the robot $(x', y')^T$ and the current estimate of the location $(\bar{\mu}_{j,x}, \bar{\mu}_{j,y})^T$ of landmark j. In this model a Gaussian noise model $\mathcal{N}(0, Q_t)$ is included with standard deviation of 15% for the measured range (σ_r)and $10 \deg$ for the bearing (σ_ϕ). Further note that for the mapping case the location of landmark j is not known (as in the localization case), but estimated.

Equation 1 and 2 define respectively the state transition function $g(u_t, x_{t-1})$ and the measurement function $h(x_t, j, m)$ of an Extended Kalman Filter. This non-linear functions can be linearized by calculating their first order partial derivatives; the Jacobian matrices G and H.

A remaining issue is need for a validation gate on the observations (as suggested by Kristensen *et. al* [4]). The validation gate is based on the innovation vector $z_t - \bar{z}_t$, which is converted to a measure for the Mahalanobis distance with aid of the overall measurement prediction uncertainty $S_t = H_t\bar{\Sigma}_t H_t^T + Q_t$, a combination of the state uncertainty $\bar{\Sigma}_t$ and the measurement uncertainty Q_t. The Mahalanobis distance is thresholded on a fixed value γ:

$$(z_t - \bar{z}_t)S_t^{-1}(z_t - \bar{z}_t)^T < \gamma \tag{3}$$

In the result section an indication of the sensitivity analysis on the actual value of γ will be given.

B. FASTSLAM 1.0

The FastSLAM algorithm was originally developed by Montemerlo *et al.*[16]. The FastSLAM algorithm is a particle filter, where each particle represents an estimate of the path

the robot has driven and an estimate of a location of each landmark. The FastSLAM algorithm maintains the landmark location estimates with a Extended Kalman Filter, with the same observation model as described in the previous section. The motion model defines a proposal distribution for the next robot location for each particle k:

$$\mu_{x_t}^{[k]} \sim \mathcal{N}(x_t, g(x_{t-1}^{[k]}, u_t), R_t) \tag{4}$$

From this distribution position are sampled. The proposed positions are checked against how probable there are according to the observation model, which determines the particle weight. The particles are resampled according to this weight. The estimates of landmark locations are independently updated, without direct correlation, although there is an indirect correlation via the robot path [17].

C. FASTSLAM 2.0

The FastSLAM 2.0 is an efficient version of the original algorithm [18]. The main improvement of FastSLAM is in shape of the initial distribution. For FastSLAM 1.0 the initial distribution was only determined by the motion model. If this distribution doesn't correspond with the observation model, many samples are rejected, which makes the algorithm inefficient. By including the observation model via the innovation vector $z_t - \hat{z}_t^{[k]}$ into the initial distribution, this distribution resembles the target distribution much better, which means that less samples have to be rejected.

$$\mu_{x_t}^{[k]} \sim \mathcal{N}(x_t, \mathcal{K}_{x_t}^{[k]}(z_t - \hat{z}_t^{[k]}) + g(x_{t-1}^{[k]}, u_t), \Sigma_{x_t}^{[k]}) \tag{5}$$

Now the initial distribution is sampled with a Gaussian with covariance $\Sigma_{x_t}^{[k]} = [H_x^T Q_t^{[k]^{-1}} H_x + R_t^{-1}]^{-1}$. The innovation vector $z_t - \hat{z}_t^{[k]}$ is incorporated in the mean of the distribution with a factor $\mathcal{K}_{x_t}^{[k]} = \Sigma_{x_t}^{[k]} H_x^T Q_t^{[k]^{-1}}$. This factor $\mathcal{K}$ has a role equivalent with the Kalman gain K in the observation model. Updating the Extended Kalman Filters for the landmarks and the resampling are performed equivalent with FastSLAM 1.0 [2].

IV. RESULTS

Gutmann *et al.* [3] recorded an extensive dataset with their Aibo ERS 2100 system. The dataset consists of 58 minutes of walking between five positions on the field. Each time such a marked position was reached, the button on the head of the Aibo was touched, with gave a "mark" in the logfile. For our analysis, we concentrated on the path between the first three marks. The path to the first mark (N=758) is illustrated in Fig. 2 in green, the path to the second mark (N=1159) is red and the path to third mark (N=1434) is blue. As can be seen from Fig. 2, the marks are not always correctly synchronized (the mark between the first and second part of the dataset seems quite late). Further note the path consists of a number of rather short turns.

Each landmark has been given a unique signature, as indicated in the legend of Fig. 2. For instance, landmark1 is the landmark in the lower right corner, indicated with
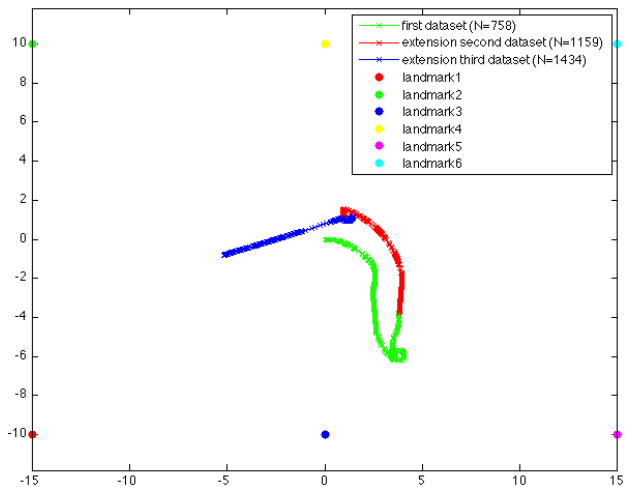

Fig. 2: The reference path between the first three marks, as calculated with the sensor resetting localization method [19].

a red marker, although the actual color coding of the tube (illustrated in Fig. 1) is the combination magneta/cyan. In the next figure the same marker color is used to show the observations made along the reference path. As can be seen, the observations have a wide spread. The bearing is sometimes 10 degrees off. The largest outliers can be found at the bottom, the red observations are nearly 45 degrees off.
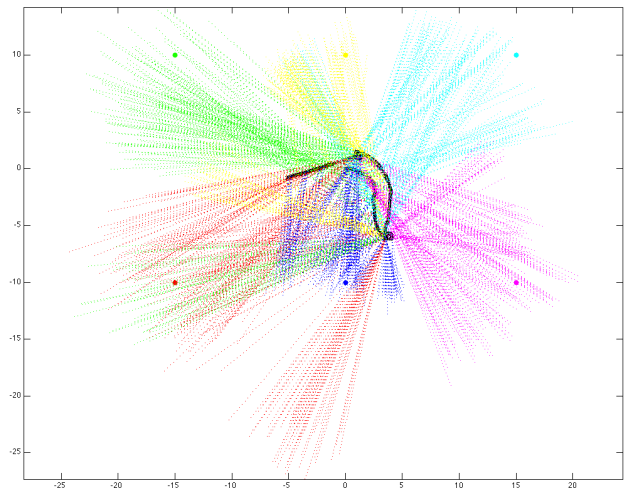

Fig. 3: The observations of the landmarks along the reference path.

Note that experiments of Gutmann *et al.* [3] were localization experiments; the location of the landmarks was precisely known. The same dataset can be used for mapping experiments, by not using this apriori information. The result can be seen in Fig. 4. This figure has been generated with the Extended Kalman Filter method described in section III-A

Note that the whole map is rotated a few degrees and shifted to the right, indicating that the location of the landmarks was not known. The only apriori data is the start pose of the Aibo. Also note that the covariance of the green upper left landmark is large, because this landmark is
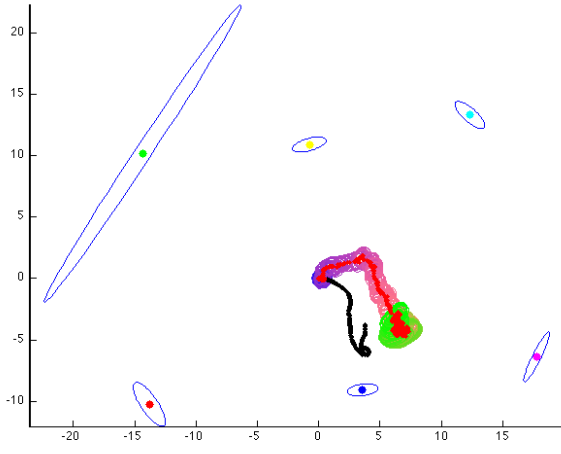
Fig. 4: The simultaneous localization and mapping result with EKF-SLAM for the first dataset (N=758).

Fig. 6: The simultaneous localization and mapping result with EKF-SLAM for the third dataset (N=1432).

not sufficiently observed when the robot is walking towards the lower right corner. Also note the ellipses around the estimated path of the robot. These ellipses indicate the confidence in the position. The uncertainty ellipses indicate the area with a probability of 0.68. The latest uncertainty estimates are green, older estimates become purple.
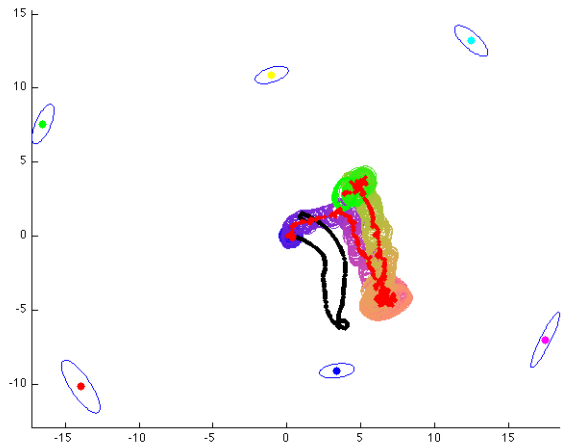

Fig. 5: The simultaneous localization and mapping result with EKF-SLAM for the second dataset (N=1159).

As can be seen in Fig. 5, the covariance of the green upper left landmark is reduced when the Aibo walks back. Also note that covariance around he position of the robot grows when the robot makes many turns, but shrinks again when the robot is walking along a straight line. The same conclusion can be drawn from Fig. 6.

These figures are the results of a sensitivity study on the parameter γ. The threshold of the validation gate γ has been varied in the range [1,5]. The value of 1.5 gives the best results. Also the noise parameters in the observation model have been varied. The variance in the range (σ_r^2) and the bearing (σ_ϕ^2) have been varied in the range [0.01,0.4]. The
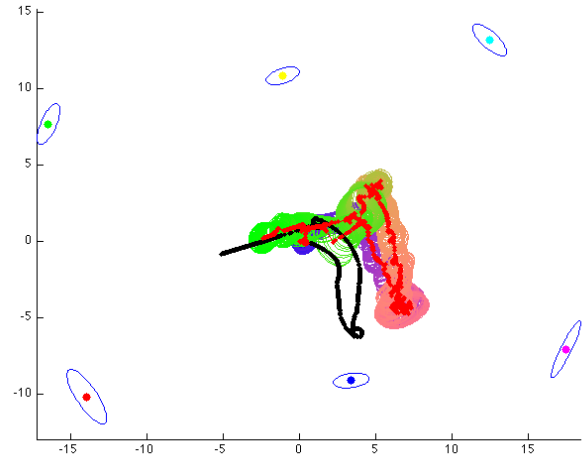
optimal results were found for the values $\sigma_r^2 = 0.17$ and $\sigma_\phi^2 = 0.38$.

A. FASTSLAM 1.0 & 2.0

For FastSLAM the results of a larger dataset were used (N=4000). The results of the EKF-SLAM algorithm are used as reference. The experiments are performed for both variants of FastSLAM: FastSLAM 1.0 and FastSLAM 2.0. For both variants also the result with stratified resampling is given. All variants shown in Fig. 7 use 100 particles. As expected outperforms FastSLAM 2.0 FastSLAM 1.0. Stratified resampling doesn't resample each timestep, but uses a measure for when to resample is the sample variance[12]. This technique makes the solution more stable, but has downside that the solution can slowly drift off. It is also clear that for this small number of landmarks the classical EKF-SLAM algorithm cannot be beaten.
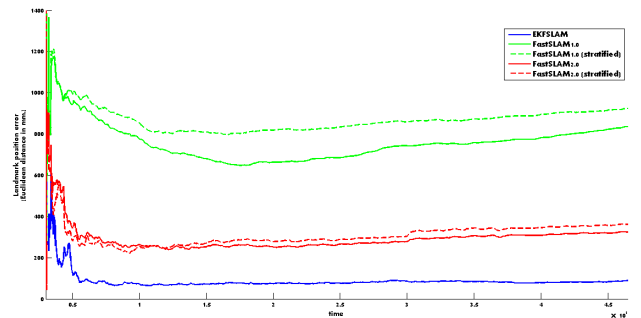

Fig. 7: A comparison of different SLAM algorithms. The measure is the distance between the estimated location of each landmark against the apriori location of each landmark.

An animation of the localization and mapping of the stratified resampling method is published on YouTube[2].

[2]http://www.youtube.com/watch?v=1fv9w53XlcQ

V. CONCLUSION

The dataset provided by Gutmann *et al.* [3] is an ideal benchmark to test different SLAM algorithms against each other. The map consists of only 6 landmarks, which prevents any scaling problems. The noise in both the motions and observations of the Aibo are challenging enough for state-of-the art algorithms as FastSLAM [17]. Although the dataset is easy to manage, still all aspects of the motion model, observation model, corresponding noise models, validation gate and resampling methods have to be carefully implemented before more complex SLAM problems can be solved.

Acknowledgement

REFERENCES

[1] S. Thrun, "Robotic Mapping: A Survey," in *Exploring Artificial Intelligence in the New Millenium*. Morgan Kaufmann, 2002.

[2] S. Thrun, W. Burgard, and D. Fox, *Probabilistic Robotics (Intelligent Robotics and Autonomous Agents)*. The MIT Press, September 2005.

[3] J.-S. Gutmann and D. Fox, "An experimental comparison of localization methods continued," in *Proceedings of the IEEE/RSJ International Conference on Intelligent Robots and Systems (IROS'02)*, October 2002.

[4] S. Kristensen and P. Jensfelt, "An experimental comparison of localisation methods, the mhl sessions," in *Proceedings of the IEEE/RSJ International Conference on Intelligent Robots and Systems (IROS'03)*, 2003.

[5] J. L. Peralta-Cabezas, M. Torres-Torriti, and M. Guarini-Hermann, "A comparison of bayesian prediction techniques for mobile robot trajectory tracking," *Robotica*, vol. 26, 2008.

[6] H. Kose, B. Celik, and H. Akin, "Comparison of localization methods for a robot soccer team," *International journal of advanced robotic systems*, vol. 3, 2006.

[7] S. Parsons, "A note on robot localization," Brooklyn College, City University of New York, January 2005.

[8] Z. Crisman, E. Curre, C. Kwok, L. Meyers, N. Ratliff, L. Tsybert, and D. Fox, "Team Description: UW Huskies-02," University of Washington, 2002.

[9] F. Dellaert, A. Kipp, and P. Krauthausen, "A Multifrontal QR Factorization Approach to Distributed Inference Applied to Multirobot Localization and Mapping," in *Proceedings of the AAAI National Conference on Artificial Intelligence*, 2005.

[10] B. Browning, M. Bowling, and M. Veloso, "Improbability filtering for rejecting false positives," in *Proceedings of 2002 IEEE International Conference on Robotics and Automation*, May 2002.

[11] Y. Bar-Shalom, X. R. Li, and T. Kirubarajan, *Estimation with Applications to Tracking and Navigation: Theory, Algorithms, and Software*. New York: Wiley, 2001.

[12] T. Bailey and H. Durrant-Whyte, "Simultaneous localization and mapping (SLAM): part II," *IEEE robotics & automation magazine*, vol. 13, 2006.

[13] M. W. M. G. Dissanayake, P. M. Newman, H. F. Durrant-Whyte, S. Clark, and M. Csorba, "A solution to the simultaneous localization and map building (slam) problem," *IEEE Transactions on Robotic and Automation*, vol. 17, pp. 229–241, 2001.

[14] P. Moutarlier and R. Chatila, "An experimental system for incremental environment modelling by an autonomous mobile robot," in *The First International Symposium on Experimental Robotics I*, ser. Lecture Notes in Control and Information Sciences, vol. 139. London, UK: Springer-Verlag, 1990, pp. 327–346.

[15] J. J. Leonard and H. F. Durrant-Whyte, "Simultaneous map building and localisation for an autonomous mobile robot," in *In IEEE/RSJ International Workshop on Intelligent Robots and Systems*, 1991, pp. 1442–1447.

[16] M. Montemerlo, S. Thrun, D. Koller, and B. Wegbreit, "Fastslam: A factored solution to the simultaneous localization and mapping problem," in *Proceedings of the AAAI National Conference on Artificial Intelligence*. Edmonton, Canada: AAAI, 2002.

[17] M. Montemerlo and S. Thrun, *FastSLAM A Scalable Method for the Simultaneous Localization and Mapping Problem in Robotics*, ser. Springer Tracts in Advanced Robotics, 2007, vol. 27.

[18] M. Montemerlo, S. Thrun, D. Koller, and B. Wegbreit, "Fastslam 2.0: An improved particle filtering algorithm for simultaneous localization and mapping that provably converges," in *Proceedings of the Sixteenth International Joint Conference on Artificial Intelligence (IJCAI)*. Acapulco, Mexico: IJCAI, 2003.

[19] S. Lenser and M. Veloso, "Sensor resetting localization for poorly modelled mobile robots," in *Proceedings of the IEEE International Conference on Robots and Automation (ICRA)*, 2000, pp. 1225 – 1232.